Comparison of the Minnaert constant for different forest types using multi-temporal SPOT/HRV data

Murakami, T.
Department of Forest and Forest Products Sciences, Faculty of Agriculture, Kyushu University
6-10-1 Hakozaki, Higashi-ku, Fukuoka, 812-8581, Japan
muratac@ffp.kyushu-u.ac.jp

Abstract: In the Minnaert topographic correction method, although the Minnaert constant should be decided for each landcover, few studies have compared how much it changes with the scene observed. Therefore, this study compared the Minnaert constants of three forest types using multitemporal remote sensing images. The Minnaert constant for each forest type was computed using sampling data for the same topographical features (*e.g.*, slope angle and slope azimuth), and tested for significant differences. Furthermore, the Minnaert constants were obtained from stratified random sampling data based on topographic features alone, without specifying the forest type, and similarities between the results were discussed. The study area was a forested area in the Sangun Mountains, in the environs of the city of Fukuoka, Japan. The satellite images consisted of SPOT/HRV data for seven scenes observed during 1997. A comparison of the Minnaert constants between the three forest types, using samples with the same topographic conditions, failed to reveal significant differences for some scenes. Additionally, the Minnaert constants for the random sampling data, based only on stratified topographic conditions, did not differ significantly in any scene or band. Consequently, even with samples stratified using topographical features, the Minnaert constant appears to be stable.
Keywords: Minnaert constant, Minnaert correction, Multi-temporal remote sensing data, SPOT/HRV, Topographic effect

1. Introduction

Almost all forests in Japan are located on sloping ground in rugged terrain. Shade caused by such topographic relief can create serious obstacles to the analysis of remote sensing data [2,8]. Since the early 1980s, various forest remote sensing studies have attempted to address this "topographic effect" problem [5,14]. Two correction methods are available to offset topographic effects: a non-geometric technique that uses band ratios and a geometric technique based on solar, surface, and sensor positions. The present study focused on the geometric technique.

Smith *et al.* [14] introduced geometric correction methods for topographic effects. The Lambert model and model correction methods that they presented continue to be cited by many researchers and a number of verification studies have been conducted. The Lambert model assumes the land surface has perfect scatter in which the bidirectional reflectance factor is independent of incidence and exitance angles. This model is very simple, dividing an observed radiation value by the cosine of a solar incidence angle. Actual land surfaces, however, seldom result in even scattering in all directions, and some researchers have noted the limitations of the Lambert model [1,9,12,15].

Another model correction method uses the Minnaert constant [14]. The value of the Minnaert constant is determined by landcover characteristics and relates to surface roughness [10,14]. Although some additional correction models incorporate the solar incidence angle [4,7,13,15], these models have not been widely used, mainly because of the complicated parameter preparation required. The Minnaert correction method is both easy to apply and theoretically linked with the Lambert model. Therefore, the Minnaert method is an appropriate correction model for topographic effects.

Murakami [11] studied seasonal variation in the Minnaert constant for three forest types (bamboo, broadleaf, and coniferous plantation forest) using multi-temporal SPOT/HRV data and discussed similarities and differences based on band variation. That study, however, lacked adequate comparison of the Minnaert constant

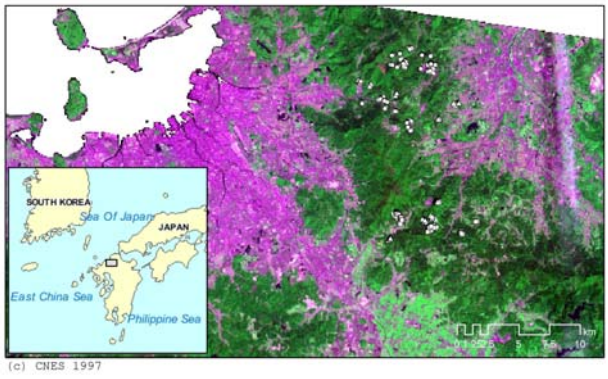

Fig. 1. Study area.

Table 1. Satellite image data list.

Observation Date	Day of the Year	Pointing Angle (deg.)
17 January 1997	17	R 7.3
5 March 1997	64	R 13.8
26 April 1997	116	R 14.1
17 June 1997	168	R 14.1
23 July 1997	204	R 0.8
25 Octorber 1997	298	R 15.2
5 December 1997	339	L 5.9

among forest types, and any change in the constant with forest type remained unclear. Because just one Minnaert constant is generally used for an entire image, it is desirable that Minnaert constants for various forest types do not differ significantly. Therefore, it is important to compare the Minnaert constant among forest types.

The present study compared Minnaert constants for different forest types using multi-temporal remote sensing data. Minnaert constants for each forest type were derived from sample data with like topographic conditions; significance tests were used to examine the results. Minnaert constants were also derived from sample data randomly stratified using only topographic conditions (slope angle and slope azimuth), without specifying forest type.

2. Materials and Methods

1) Study area

Two study sites were selected in a forested area of the Sangun mountainous region near Fukuoka, Japan (Fig. 1). Elevations in this area range from 30 to 930 m above sea level, and the natural vegetation is warm-temperate evergreen broadleaf forest. Secondary natural broadleaf forest presently dominates the area. Other landcover includes coniferous plantation forests composed mainly of Japanese cedar (*Cryptomeria japonica*) and Japanese cypress (*Chamaecyparis obutusa*) and bamboo forests.

2) Data and preprocessing

Seven SPOT/HRV images were analyzed (Table 1). All SPOT/HRV data were observed in 1997. SPOT/HRV has three bands: band 1 (visible green, 500–590 nm), band 2 (visible red, 610–680 nm), and band 3 (near-infrared, 790–890 nm). The spatial resolution of SPOT/HRV is 20 m.

A 50-m grid digital map published by the Geographical Survey Institute of Japan was used for the digital elevation model (DEM). This DEM was applied for the geometric registration (including ortho-rectification) of satellite data and for the calculation of the solar incidence angle and sensor exitance angle in each pixel. A 1:25000 digital map produced by the Geographical Survey Institute was used for geometric registration.

ERDAS IMAGINE software Version 8.7 (Leica Geosystems Geospatial Imaging, Norcross, GA, USA) was used for preprocessing the satellite data. All data were geometrically registered on a Universal Transverse Mercator projection, zone 52. The SPOT model of ERDAS IMAGINE, one of the specific rectification modules, was applied to correct topographic distortion resulting from the central projection and oblique viewing. Atmospheric correction was not conducted to avoid the error caused by this correction process and because only relative variation information was required.

3) Minnaert constants

The Minnaert correction method is one of the most common topographic correction methods [14] . This model is based on an empirical formula originally proposed by Minnaert [10]. Smith *et al.* [14] adopted the Minnaert constant to correct topographic effects and further research has confirmed its effectiveness [1,9,15]. The Minnaert method is expressed by the following formula:

$$Dc = \frac{Do \cdot \cos \varepsilon}{(\cos i \cdot \cos \varepsilon)^k} \quad (1)$$

where Dc is the corrected data value, Do is the original data value, i is the solar incidence angle, ε is the sensor exitance angle, and k is the Minnaert constant.

The solar incidence angle is defined as the position of the Sun with respect to the surface normal. Parameters related to topographic conditions (slope angle and slope azimuth) and solar position (solar zenith angle and solar azimuth) are required for determining the solar incidence angle as follows:

$$\cos i = \cos \theta \times \cos e + \sin \theta \times \sin e \times \cos (\varphi - A) \quad (2)$$

where e is the slope angle, φ is the slope azimuth, θ is the solar zenith angle, and A is the solar azimuth. The sensor exitance angle is similarly defined as the angle between the surface normal and the sensor position. Solar position is often replaced by sensor position for the above-mentioned solar incidence angle calculation. The sensor exitance angle is defined as:

$$\cos \varepsilon = \cos \gamma \times \cos e + \sin \gamma \times \sin e \times \cos (\varphi - \psi) \quad (3)$$

where γ is the sensor zenith angle and ψ is the sensor azimuth. For the oblique viewing of SPOT/HRV, the sensor

Table 2. The solar and sensor positions at the time of the satellite observations.

Observation date	Solar zenith angle (deg.)	Solar azimuth (deg.)	Sensor zenith angle (deg.)	Sensor azimuth (deg.)
17 January 1997	57.72	157.29	8.26	101.12
5 March 1997	44.68	148.48	15.64	101.75
26 April 1997	26.04	136.18	15.98	101.78
17 June 1997	19.46	116.72	15.98	101.78
23 July 1997	21.17	124.94	0.90	100.52
25 Octorber 1997	47.76	160.35	17.23	101.89
5 December 1997	55.63	164.66	6.67	280.99

exitance angle may vary with the scene. Table 2 shows the four required parameters for the solar incidence angle.

After logarithmic transformation of Equation 1, as follows, the Minnaert constant is determined as the slope of linear regression:

$$\ln(Do \cdot \cos\varepsilon) = k \cdot \ln(\cos i \cdot \cos\varepsilon) + \ln(Dc) \quad (4)$$

The correction of topographic effects can be achieved by substituting parameter k in Equation 1. In this analysis, Do was the value that converted the digital number to radiance. The radiance conversion factors were derived from a header file attached to the SPOT/HRV data.

4) Data sampling methods

Smith *et al.* [14] suggested that the Minnaert constant is inherent to a landcover type, meaning that the landcover type must be spatially explicit prior to calculating the Minnaert constant. Therefore, a previously classified remotely sensed image or specific GIS data for a given area must already exist. However, if such data pre-exist, there is little need for correction of topographic effects. For cases with no prior data available, it is desirable to examine the difference of Minnaert constants among forest types and validate the consistency of Minnaert constants derived without specifying forest type. Thus, in the present study, sample data were extracted using the following procedures and the resulting Minnaert constants were statistically compared.

I. The sample points for each forest type were established by comparing a vegetation map published by the Environment Agency of Japan with satellite data. Comparisons accounted for any changes that may have occurred between the date of the map (1988) and the satellite data observation year (1997). Furthermore, because distinguishing forest types based only on a single SPOT/HRV image was difficult, two or more images were combined to improve the visual interpretation. Combining scenes allowed for effective discrimination of the three forest types. The combination of band 3 in April (day of year [DOY] 116) and June (DOY 168) resulted in the very accurate identification of broadleaf, coniferous, and bamboo forests. After ensuring that there were no clouds or cloud shadows over the sampling point for each scene, the sampling point was established. This method was used to create the primary dataset.

II. As noted above, the Minnaert constant tends to be affected by sampling bias because the constant is derived from regression analysis. To avoid topographic bias in the sample data, Murakami [11] used stratified random sampling to extract sample data based on a combination of topographical features (slope angle and slope azimuth). In this study, the sampling design was adjusted so that only data related to the combination of slope angle and slope azimuth would be extracted for each forest type.

III. The first objective of this study was to compare Minnaert constants among forest types; the data were author-controlled so that the sampling conditions of the three forest types would be standardized. Accordingly, the extracted data for the three forest types had the same combinations of slope angle and slope azimuth. The sample set obtained using this method was called Sample I.

IV. Other data were extracted without specifying forest type, although the data had to represent one of the three target forest types. This dataset, which consisted of topographic data (slope angle and slope azimuth from the DEM) and satellite data (the digital number [DN] of each band), was extracted from a forest-covered mountainous area. Stratified random sampling based on topographical conditions was then conducted. Stratification criteria included slope angle and slope azimuth. For stratification, classes were established at combinations of 5° intervals (0–40°) for slope angle and 15° intervals for slope azimuth; classes expressed similar topographic units. One sample (the set of topographic and satellite data) was randomly extracted per class. It was assumed that topographic bias was eliminated through this sampling method. To validate the stability of the Minnaert constant, these operations were repeated 10 times. Ten Minnaert constants were calculated per scene and per band and were compared using statistical tests. The sample dataset compiled using this process was referred to as Sample II.

5) Statistical test

Because a Minnaert constant is the slope of a regression line, comparing Minnaert constants means comparing the slopes of regression lines. A test of parallelism of covariance analysis (ANCOVA) was used to compare the slopes of the regression lines. In this analysis, a test of significant difference in the Minnaert constants was carried out using a test of parallelism. The statistical analysis software R 1.9.1 (http://www.r-project.org/) was used for this test.

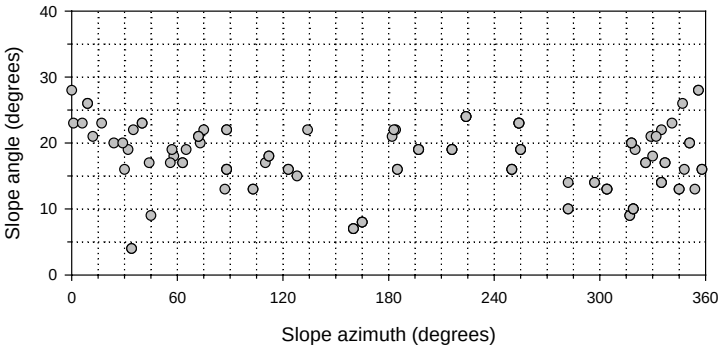

Fig. 2. Scattergram between slope azimuth and slope angle for the analysis of Sample I.

3. Results

Figure 2 shows a scattergram of Sample I. For slope angle, the points concentrated between 10 and 30°. Relatively few samples, however, had a slope azimuth of 150–270°. Although extracted data did not scatter equally for all topographic features, the main purpose here was obtaining the same topographical features for the three forest types. Thus, the following analysis comparing the Minnaert constants among forest types could be carried out using Sample I.

Figure 3 shows the results of Sample I analysis. Figure 3a focuses on band 1, which had a convex-shaped overall change pattern. The broadleaf forest had the largest value throughout the year. When the Minnaert constants for each forest type were compared for each scene, a difference exceeding 0.1 was only found on DOY 116 (0.103). Differences for the other scenes ranged from 0.090–0.011. The minimum difference occurred on DOY 17. As illustrated in Fig. 3b, the seasonal variation pattern for band 2 was similar to that for band 1. The largest difference, 0.120, occurred on DOY 116, and the next greatest difference was on DOY 64 (0.110). Other scenes had differences of less than 0.1. Band 3 differed slightly from bands 1 and 2 in that its seasonal variation pattern varied within a certain range rather than forming a clear peak (Fig. 3c). Moreover, although the broadleaf forest had the highest value for bands 1 and 2, no clear ranking of forest types was found for band 3. The maximum difference in band 3 was 0.132 (DOY 116), followed by 0.129 (DOY 64). The minimum difference was 0.032 (DOY 168). In general, differences in the Minnaert constants for band 3 were larger than those for bands 1 and 2.

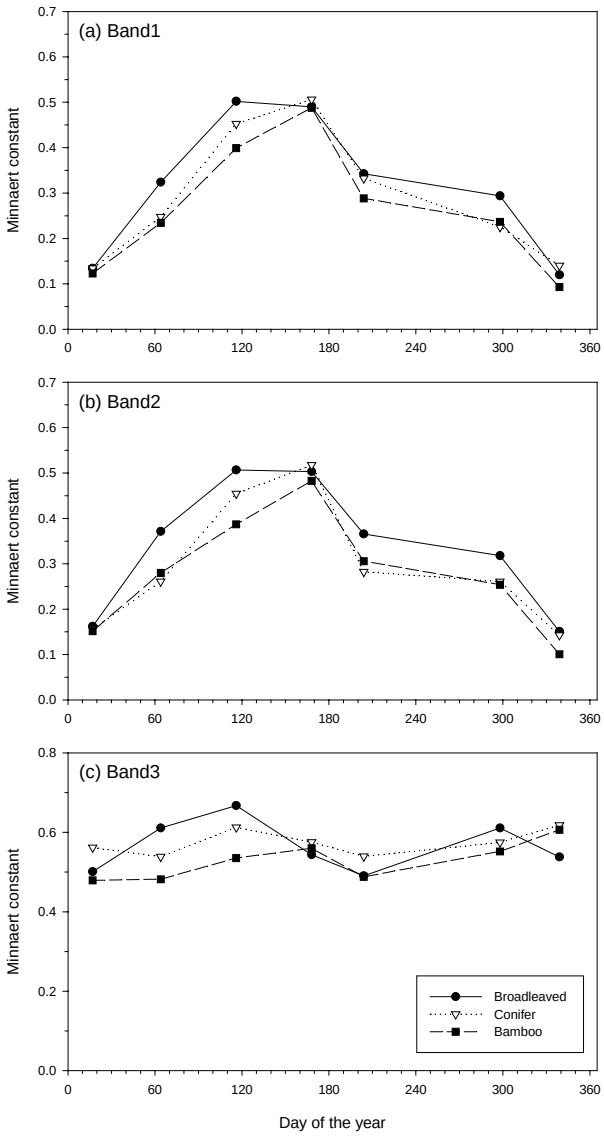

Fig. 3. The Minnaert constants for three forest types derived from same topographical features. (a) Band 1, (b) Ba-nd 2, and (c) Band 3.

Table 3 shows the results of significance tests on Minnaert constants by forest type for each scene. The values in this table indicate significance probability. For band 1, no significant difference was recognized in the Minnaert constants of the three forest types on DOY 168, 204, and 298. For band 2, only DOY 298 had no significant difference. Band 3 had the most scenes without significant difference. Five of the seven scenes had no significant difference in Minnaert constants among the three forest types.

Figure 4 shows the scattergram of one set of SPOT/HRV-derived sample data. Almost all topographic conditions were represented by uniform amounts of data. Thus, for the stratification of topographic conditions, data were randomly sampled, and Minnaert constants were calculated.

Figure 5 illustrates seasonal variations in Minnaert constants for each band, as shown by mean values and standard deviations. Variation in the Minnaert constant was small for band 1 (±0.003–0.006 SD). The variation for band 2 was similar to that for band 1 (±0.005–0.009 SD). Band 3 had standard deviations larger than those for bands 1 and 2 (±0.015–0.022 SD). Table 3

Table 3. Significant probability of the parallelism test. The results for Minnaert constants obtained from the Sample I.

	Day of the Year						
	17	64	116	168	204	298	339
Band1	0.000**	0.000**	0.000**	0.120	0.532	0.062	0.000**
Band2	0.000**	0.000**	0.004**	0.029*	0.000**	0.056	0.000**
Band3	0.121	0.190	0.000**	0.010**	0.331	0.429	0.112

** significant at the 0.01 level, * significant at the 0.05 level

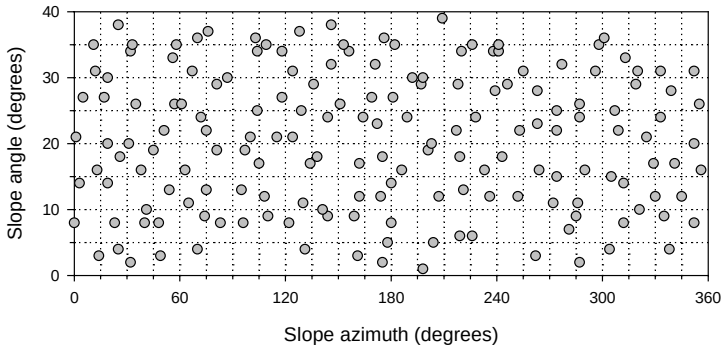

Fig. 4. Scattergram between slope azimuth and slope angle for the analysis of Sample II.

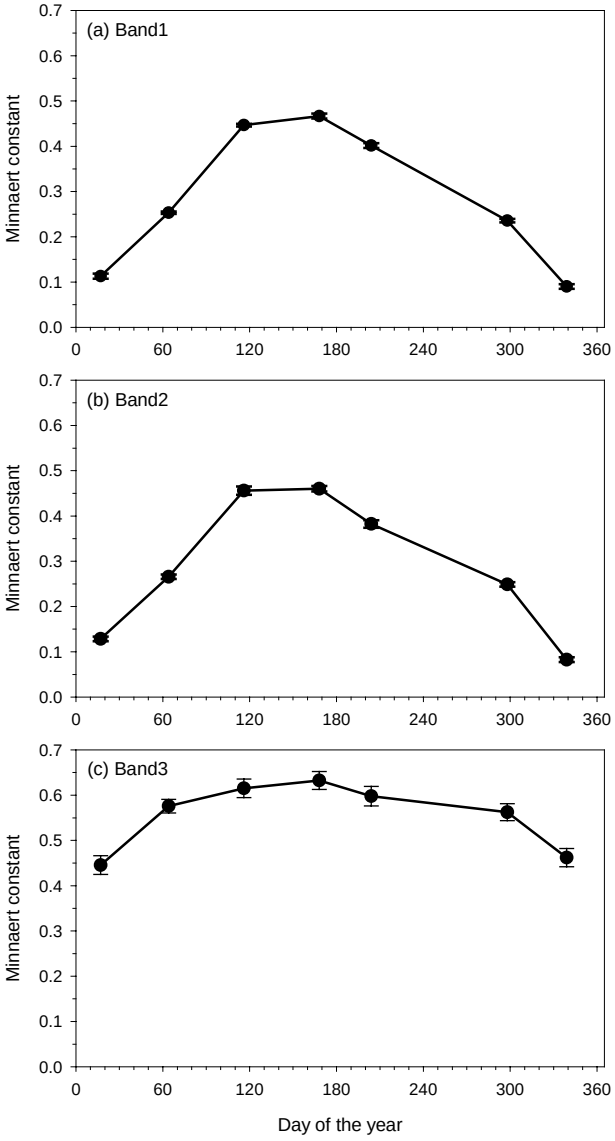

Fig. 5. The Minnaert constants derived from stratified random sampling, Sample II. Error bars represent standard deviations. (a) Band 1, (b) Band 2, and (c) Band 3.

Table 4. Significant probability of the parallelism test. The results for Minnaert constants obtained from SampleII.

Observation date	Band1	Band2	Band3
17 January 1997	0.936	0.948	0.621
5 March 1997	0.999	0.999	0.944
26 April 1997	0.999	0.981	0.962
17 June 1997	0.937	0.985	0.996
23 July 1997	0.999	0.999	0.998
25 October 1997	0.999	0.998	0.916
5 December 1997	0.989	0.974	0.814

summarizes the significance test results. The values in this table show the probability of Minnaert constant similarity. All dates and bands indicated no significant differences. The SPOT/HRV dataset showed that the Minnaert constants obtained from samples stratified using topographic conditions were stable.

4. Discussion

Seasonal variation of the Minnaert constant was examined as an aspect of the comparison of Minnaert constants among the three forest types. Variation was investigated for both single and two or more scenes. Minnaert constants for each forest type based on data with the same topographical conditions showed no significant difference for some scenes or bands (Fig. 3 and Table 3). Furthermore, Minnaert constants derived only from topographic conditions without forest-type specification presented no significant difference in all bands and all scenes (Fig. 5 and Table 4). While not directly confirming that Minnaert constants are similar regardless of forest type, combined with results of a former study conducted in the suburbs of the study area, these results suggest that a stable Minnaert constant can be obtained taking only topographic conditions into consideration. Obtaining Minnaert constants for each forest type is difficult, and applying more than one constant to a scene is impractical. Therefore, the indication that Minnaert constants can be determined without considering forest type is important.

In comparison with Sample II (Fig. 5), which was stratified only by topographical conditions without specifying forest types, Sample I (Fig. 3), based on topographic conditions alone, had larger variation in the value of Minnaert constants. This difference probably reflects deviations caused by the geographical features. Moreover, in Sample I (Fig. 3), seasonal variations in the Minnaert constants were somewhat irregular, while those for Sample II (Fig. 5) showed a smooth curve; deviation caused by topographical conditions may also be reflected in these results. In Sample II (Fig. 5), no significant difference was recognized even after changing the dataset combination used to calculate the Minnaert constant. This result suggests the importance of stratification based on topographical conditions.

Previous studies have calculated Minnaert constants from single scenes [3,4,9,14,15] or a few separate scenes [5,2]. Moreover, it is unknown how much these studies considered biases caused by topographic conditions. As demonstrated in this study, it is necessary to include topographic conditions when calculating the Minnaert constant (Figs. 2 and 4). Taking all topographic conditions into consideration (*i.e.*, the slope azimuth and slope angle) is both logical and important because the Minnaert constant depends on regression analysis. As the analysis results of this study show, a highly stable solution results if almost all topographic conditions are considered.

At present, the applicability of our results is limited. In the study area in the northern part of the Kyushu District, warm temperate forests composed mainly of evergreen species dominate. In more northern regions and at higher elevations where deciduous forests dominate, it is unknown whether a stable Minnaert constant can be achieved. Unlike evergreen forests, deciduous forest experience dramatic changes in spectral reflectance characteristics due to leaf color change and drop. Future research should apply the same approach to other areas to examine the stability of the Minnaert constant.

Furthermore, this study only examined SPOT/HRV-derived data. Additional analysis should use middle-resolution satellite data such as that obtained by LANDSAT/TM and Terra/ASTER. As shown by Sample II in the present study, sampling without specifying a forest type can be effective. One advantage of this approach is that it only requires image data and a DEM, not prior or additional information. This method is thus simple and easy to use as an initial analysis. In addition, this study demonstrated the stability of the Minnaert constant through significance tests and indirectly clarified whether the Minnaert constant varies with forest type. If established methods to acquire the Minnaert constant existed for any sensor or area, topographic effect correction processes would progress greatly.

Acknowledgment

The SPOT/HRV data used in this study were provided by the National Space Development Agency of Japan (Japan Aerospace Exploration Agency).

References

[1] Chiou, C.R., Thomas, V.L., and Hoffer, R.M. (1992) Comparison of four techniques for topographic normalization of Landsat TM data, *ASPRS/ACSM/RT 92-Technical Papers* 4: 184-196.

[2] Civco, D.L. (1989) Topographic normalization of Landsat Thematic Mapper digital imagery, *Photogramm. Eng. Remote Sens.* 55: 1303-1309.

[3] Colby, J.D. (1991) Topographic normalization in rugged terrain, *Photogramm. Eng. Remote Sens.* 57: 531-537.

[4] Gu, D., and Gillespie, A. (1998) Topographic normalization of Landsat TM images of forest based on subpixel sun-canopy-sensor geometry, *Remote Sens. Environ.* 64: 166-175.

[5] Holben, B., and Justice, C. (1980) The topographic effect on spectral response from nadir-pointing sensors, *Photogramm. Eng. Remote Sens.* 46: 1191-1200.

[6] Holben, B., and Justice, C. (1981) An examination of spectral band ratioing to reduce the topographic effect on remotely sensed data, *Int. J. Remote Sens.* 2: 115-133.

[7] Kawata, Y., Ueno, S., and Kusaka, T. (1988) Radiometric correction for atmospheric and topographic effects on Landsat MSS images, *Int. J. Remote Sens.* 9: 729-748.

[8] Leprieur, C.E., Durand, J.M., and Peyron, J.L. (1988) Influence of topography on forest reflectance using Landsat Thematic Mapper and digital terrain data, *Photogramm. Eng. Remote Sens.* 54: 491-496.

[9] Meyer, P., Itten, K.I., Kellenberger, T., Sandmeier, S., and Sandmeier, R. (1993) Radiometric corrections of topographically induced effects on Landsat TM data in an alpine environment, *ISPRS J. Photogramm. Remote Sens.* 48: 17-28.

[10] Minnaert, M. (1941) The reciprocity principle in lunar photometry, *The Astrophy. J.* 93: 403-410.

[11] Murakami, T. (2002) Minnaert constant of several forest types from SPOT/HRV data, *J. Jpn. Soc. Photogramm. Remote Sens.* 41(1): 47-55. (in Japanese with English abstract)

[12] Murakami, T., Fujii, H., and Imada, M. (1998) Comparison of correction methods for topographic effects on Landsat TM data, *Bullt. Kyushu Univ. For.* 78: 13-28. (in Japanese with English abstract)

[13] Richter, R. 1997. Correction of atmospheric and topographic effects for high spatial resolution satellite imagery, *Int. J. Remote Sens.* 18: 1099-1111.

[14] Smith, J.A., Lin, T.L., and Ranson, K.J. 1980. The Lambertian assumption and Landsat data, *Photogramm. Eng. Remote Sens.* 46: 1183-1189.

[15] Teillet, P.M., Guindon, B., and Goodenough, D.G. 1982. On the slope-aspect correction of multispectral scanner data, *Can. J. Remote Sens.* 8: 84-106.